# Instability of continuous waves and rotating solitons in waveguide arrays

S. Darmanyan,* I. Relke, and F. Lederer†
*Institut für Festkörpertheorie und Theoretische Optik, Friedrich-Schiller Universität Jena, Max-Wien Platz 1, D-07743 Jena, Germany*
(Received 20 December 1996)

The effect of a nonvanishing transverse wave vector on the stability of continuous waves and temporal solitons which propagate in an array of nonlinear optical waveguides is studied both analytically and numerically. We derive analytical expressions for the domain of existence as well as the gain of modulational instability of moving continuous waves. Because the transverse wave vector controls the ''discrete diffraction'' the stability behavior critically depends on this quantity. By employing the perturbation theory near neutrally stable modes it is shown that there are two different scenarios for the evolution of modulationally unstable soliton arrays. The transverse wave vector of the unstable solution determines which kind of instability develops. Numerical calculations confirm the analytical results. [S1063-651X(97)01606-1]

PACS number(s): 42.81.Qb, 03.65.Ge, 42.81.Dp

## I. INTRODUCTION

Nonlinear evolution equations arise in many branches of modern science. Stationary solutions to these equations can frequently be found by using both analytical and numerical methods. One of the fundamental problems left is to check these solutions against their stability, which is essential from a basic point of view as well as for potential applications, see, e.g., [1–7], and the references therein. In particular, in nonlinear optics this question has attracted a considerable amount of interest during the past several years. Different kinds of instability may lead to such phenomena as bistability, self-oscillation, and the formation of static or moving patterns. A prominent example is modulational instability (MI), which is the prerequisite for the formation of spatial or temporal patterns. In an optical fiber where the field evolution is described by the nonlinear Schrödinger equations (NLSE) MI of a continuous wave (cw) can be employed for the generation of pulse trains with a high repetition rate [8,9]. Moreover, it has been shown that recurrence phenomena and the existence of localized excitations in discrete systems can be attributed to MI of stationary solutions of the respective nonlinear equations [10,11]. It turned out that a particular feature of these systems consists in the critical dependence of both the MI gain (instability increment) and the domain of MI on the wave number of the stationary solution.

Recently it was pointed out that arrays of nonlinear waveguides represent an ideal laboratory for the study of the dynamical behavior of discrete systems [12–24]. Besides this basic point of view these arrays may be envisaged as potential all-optical devices such as, e.g., switches, or steering or logical elements. Moreover, if dispersion acts in the waveguides, arrays own the properties of both discrete and continuous systems. Thus the study of their nonlinear behavior is of fundamental interest as well. In particular, the study of discrete solitary wave solutions which represent a balance between coupling (or ''discrete diffraction'') and self-phase modulation in nonlinear optical waveguide arrays (NOWA) has attracted a considerable amount of interest. The existence of this type of localized solutions was predicted first for focusing Kerr nonlinearities [12]. As a consequence of the fact that in NOWAs the ''diffraction'' can also be negative (depending on the transverse wave vector) bright solitary waves were also found in defocusing nonlinearities [13]. These solitary waves describe either a strong (in a few waveguides) or a weak localization (minor changes from guide to guide) of the optical field in the array. The latter case leads to the continuous NLSE in the long-wavelength approximation which exhibits genuine spatial soliton solutions. A detailed evaluation of various approaches toward an analytical description of NOWAs (including also the intermediate case of localization) can be found in [14], where propagation, steering, localization, and collision effects of the solitary wave solutions are investigated. Power controlled switching in NOWAs was numerically observed in [15]. The possibility to control the propagation direction and the output channel by an initial phase tilt was shown in [16,17]. The influence of the inhomogeneity of the coupling strength in a NOWA on solitary wave formation and switching was studied in [18,19].

Recently the existence and stability of solitary wave solutions localized both temporarily and across the array were considered in [20–24]. In particular, MI of cw as well as temporal soliton solutions in NOWAs was studied in [22] where particular emphasis was paid to temporal compression and spatial localization effects. However, the authors restricted the study to the case where the transverse wave number vanishes. This means that the cw solution does not move across the array and the solitons have both the same shape and phase in all waveguides. In view of what was said above, the transverse wave number of the stationary solutions may represent an important control parameter with regard to both the MI gain and domain. Therefore the aim of this paper is to study MI for plane waves moving across the array as well as soliton solutions the phase of which rotates across the NOWA. We will term the latter solutions rotating solitons. Moreover, we will check our analytical results beyond the onset of instability by numerical means in order to identify temporal and spatial patterns, which are eventually formed.

*Permanent address: Institute of Spectroscopy, RAS Troitsk 142092, Moskow Region, Russia.
†Electronic address: pfl@uni-jena.de

 

The normalized slowly varying envelopes of the optical field in a fiber or channel waveguide array may be described by the dimensionless linearly coupled nonlinear equations [22] which can likewise be considered as mixed discrete-continuous nonlinear Schrödinger equations (DCNLSE)

$$i\partial_z U_n+\frac{\beta}{2}\partial_{tt}U_n+f(U_{n+1}+U_{n-1})+|U_n|^2U_n=0,$$

$$n=1,2,\ldots,N \tag{1}$$

where $z$ is the propagation distance scaled by the dispersion length $L_d=T_0^2/|D|$ ($D$ is the group velocity dispersion), and $t$ is the time in the reference frame of the pulse scaled by the pulse length $T_0$. The linear coupling parameter is defined as $f=\pi L_d/2L_h>0$ where $L_h$ is the half beat length of a dual core coupler. $\beta=1$ or $-1$ stands for anomalous ($D<0$) or normal ($D>0$) group velocity dispersion, respectively. The normalized amplitude $U$ is related to the slowly varying envelope of the optical field $A$ by $U=\sqrt{\gamma L_d}A$ where $\gamma$ is the effective nonlinear coefficient [7]. We note that Eq. (1) holds likewise in short arrays formed by film waveguides. There, $t$ represents a transverse coordinate scaled by the beam width $w_0$ and $L_d=\pi {w_0}^2/\lambda$ is then the diffraction length. In what follows we study the stability of two solutions to Eq. (1), viz., a moving plane wave and a rotating temporarily localized solution.

## II. MODULATIONAL INSTABILITY OF MOVING PLANE WAVES

The moving cw solution to Eq. (1) may be written as

$$U_n(z,t)=U_0e^{i(kz+qn-\omega t)}, \tag{2}$$

where $q$ is the arbitrary transverse wave vector and $\omega$ the deviation from the carrier frequency. The longitudinal wave vector component reads as

$$k=|U_0|^2+2f\cos q-\frac{\beta}{2}\omega^2.$$

We note that the linear version of this dispersion relation indicates that the transverse coupling in the array may be interpreted as discrete ''diffraction.'' Thus this diffraction resembles the continuous one (positive diffraction) only for $0\leqslant q<\pi/2$. For $q=\pi/2$ the diffraction disappears and gets negative for $\pi/2<q\leqslant\pi$. Based on this interpretation it can be anticipated that the transverse wave vector considerably affects the stability behavior of the stationary solutions.

We perform the familiar linear stability analysis [6,7] by modulating the unperturbed amplitude $U_0\rightarrow U_0+\Psi_n(z,t)$ in Eq. (2) where

$$\Psi_n(t,z)=Ae^{i(Kz+Qn-\Omega t)}+B^*e^{-i(K^*z+Qn-\Omega t)}. \tag{3}$$

Inserting Eq. (2) into Eq. (1) we get a dispersion relation for the perturbations with the amplitudes $A$ and $B$:

$$(K+\beta\omega\Omega+2f\sin Q\sin q)^2=F(F-2U_0^2), \tag{4}$$

where

$$F(\Omega,q,Q)=\frac{\beta}{2}\Omega^2+4f\cos q\sin^2\frac{Q}{2}. \tag{5}$$

It is evident that the stationary solution (2) is modulationally unstable (exponential growth of the perturbation) if the right-hand side of Eq. (4) is negative. Obviously, the gain of instability

$$\text{Im}\ [K]\equiv P=\sqrt{F(2U_0^2-F)}>0 \tag{6}$$

varies with the wave number $q$ of the stationary solution and the frequency $\Omega$ and wave number $Q$ of the perturbation, see Eqs. (4) and (5). In contrast, the real part of $K$ additionally depends on the frequency $\omega$.

The distinctive feature of discrete systems, viz., the dependence of the gain $P$ on the wave number of the stationary solution [10,11], can be clearly seen by inspecting Eq. (5). It follows from Eq. (6) that regardless of the sign of dispersion ($\beta=\pm1$) MI occurs for

$$0<F<2U_0^2, \tag{7}$$

and the maximum gain $P_{\max}=U_0^2$, which appears for $F=U_0^2$, depends only on the amplitude of the stationary solution.

Some familiar limiting cases can be read off from Eqs. (4)–(7) as MI of (i) the nonlinear Schrödinger equation [6,7] for $f\cos q=0$ (diffractionless case), (ii) the discrete nonlinear Schrödinger equation for $\beta=0$ (dispersionless case) [10], and (iii) the DCNLSE (1) for $q=0$ (zero transverse wave vector) [22].

It is obvious that the existence criterion, the domain, and the gain of MI are essentially determined by $F(\Omega,q,Q)$ which, in turn, critically depends on the sign of both $\beta$ and $\cos q$, see Eq. (5). For $\beta=-1$ (normal dispersion) and $\pi/2\leqslant q\leqslant\pi$ (zero and ''negative'' discrete diffraction) there is no MI. In what follows we study the three cases where MI may appear in detail.

(1) $\beta=1$ (anomalous dispersion) and $0\leqslant q\leqslant\pi/2$ (zero or positive ''diffraction'').

From Eq. (7) we can immediately derive the frequency range $\Omega_-<\Omega<\Omega_+$,

$$\Omega_\pm=\pm2\sqrt{U_0^2-2f\cos q\sin^2\frac{Q}{2}},$$

where MI appears. The respective domain of MI is shown in the $\Omega$-$Q$ plane for four different transverse wave vectors $q$ in Fig. 1. As usual only the first Brillouin zone is displayed. Two conclusions can be drawn from Fig. 1, viz., (i) if $2f\cos q\leqslant U_0^2$ (weak diffraction) the whole Brillouin zone is modulationally unstable and (ii) if $U_0^2<2f\cos q$ (strong diffraction) the region of MI is situated between $\pm Q_0$ with

$$Q_0=2\arcsin\left(\frac{U_0}{\sqrt{2f\cos q}}\right). \tag{8}$$

Thus on the one hand a nonvanishing transverse wave vector $q$ increases the MI domain (the short dashed line corresponds to the case studied in [22]) but on the other hand the maximum frequency does not depend on $q$.

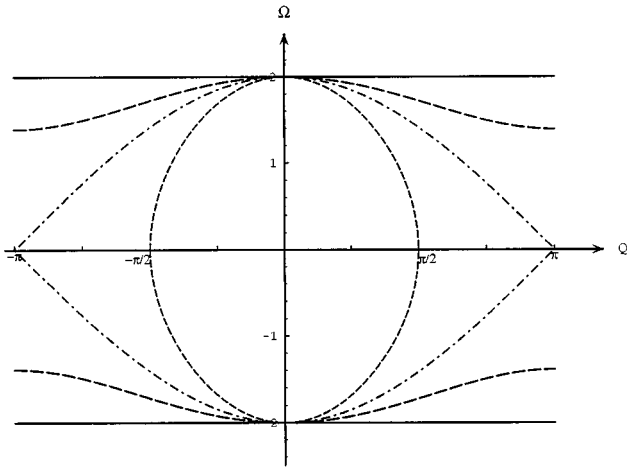


FIG. 1. The MI domain in the $\Omega$-$Q$ plane. Parameters: $U_0=f=1$, $\beta=1$, and $q=\pi/2$—solid line, $q=5\pi/12$—long dashed line, $q=\pi/3$—dashed-dotted line, $q=0$—short dashed line.

In Fig. 2 the MI gain $P$, Eq. (6), is sketched as a function of both the frequency $\Omega$ and the transverse wave vector $Q$ of the perturbation where $q=\pi/3$ (dash-dotted line in Fig. 1).

(2) $\beta=1$ (anomalous dispersion) and $\pi/2\leqslant q\leqslant\pi$ (zero or negative ''diffraction'').

In this case the MI domain is located between the frequencies $\Omega_l<|\Omega|<\Omega_u$ where

$$\Omega_u=2\sqrt{U_0^2+2f|\cos q|\sin^2\frac{Q}{2}}$$

and

$$\Omega_l=2\sin\frac{Q}{2}\sqrt{2f|\cos q|}.$$

In contrast to the former case, the MI domain always extends over the whole Brillouin zone. Furthermore, the instability region is restricted with respect to $\Omega$ and for $Q\neq 0$ separated from the frequency of the stationary solution (see Fig. 3).

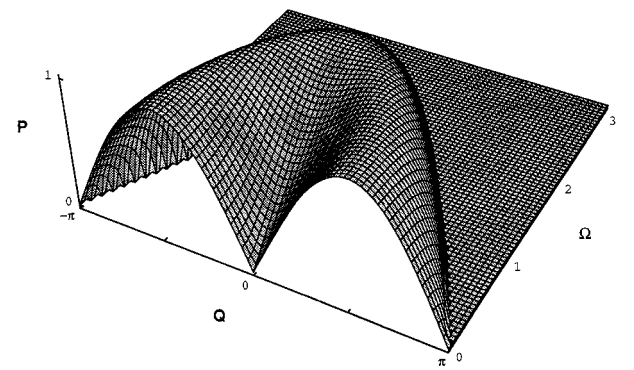


FIG. 2. The MI gain $P$ as a function of the frequency and the wave vector of the perturbation. Parameters: $U_0=f=1$, $\beta=1$, $q=\pi/3$.

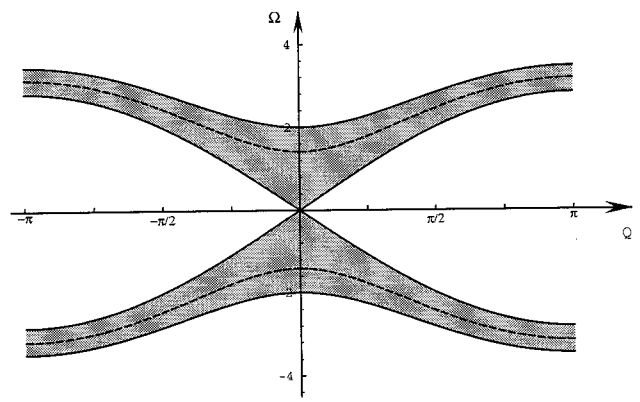


FIG. 3. The MI domain (shaded area) in the $\Omega$-$Q$ plane. Parameters: $U_0=f=1$, $\beta=1$, $q=\pi$. The dashed line indicates the maximum gain.

(3) $\beta=-1$ (normal dispersion) and $0\leqslant q<\pi/2$ (positive ''diffraction''). Here the boundaries of the MI domain are given by $\Omega_l<|\Omega|<\Omega_u$ where

$$\Omega_u=2\sin\frac{Q}{2}\sqrt{2f\cos q},$$

$\Omega_l=0$ for $2f\cos q\leqslant U_0^2$, and $\Omega_l=2\sqrt{2f\cos q\sin^2(Q/2)-U_0^2}$ for $2f\cos q>U_0^2$.

As in case (2), the MI domain always extends over the whole Brillouin zone. But in contrast to the previous case, the instability region is separated from the frequency of the stationary solution only if $2f\cos q>U_0^2$ and for $|Q|>Q_0$, where $Q_0$ is determined by Eq. (8) (see Fig. 4).

## III. MODULATIONAL INSTABILITY OF ROTATING SOLITONS

Besides the cw solution Eq. (1) exhibits a temporarily localized solution with a rotating phase as

$$u_n=g\left(t-\frac{z}{v}\right)e^{i(kz+qn-\omega t)}, \tag{9}$$

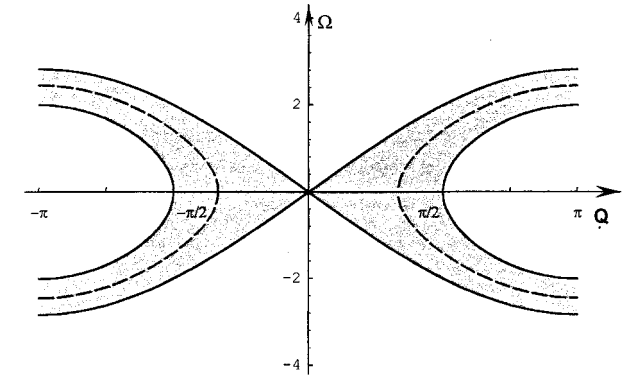


FIG. 4. The MI domain (shaded area) in the $\Omega$-$Q$ plane. Parameters: $U_0=f=1$, $\beta=-1$, $q=0$. The dashed line indicates the maximum gain.

where $v^{-1}=-\beta\omega$ is the deviation from the inverse group velocity and $g$ obeys the equation

$$\frac{\beta}{2}g''-\frac{\lambda^2}{2}g+g^3=0, \tag{10}$$

with $\lambda^2=2k+\beta\omega^2-4f\cos q>0$.

In what follows we restrict ourselves to $\beta=1$ (anomalous dispersion). Then the solution to Eq. (10) is $g=\lambda\ \mathrm{sech}\ [\lambda(t-z/v)]$. Thus Eq. (9) represents an array of solitons with equal shape, but rotating phase. The rotation is determined by the transverse wave vector $q$. To perform the linear stability analysis we make the substitution $g\to g+a+ib$ in Eq. (9) and insert this perturbed solution into Eq. (1). By linearizing the equations obtained with respect to $a$ and $b$ and by performing the Fourier transformation of $a$ and $b$ with respect to the discrete variable we arrive at

$$a_\xi+2iaf\sin q\sin Q-\hat{L}_{0f}b=0,$$

$$b_\xi+2ibf\sin q\sin Q-\hat{L}_{1f}a=0. \tag{11}$$

Here we used the reference frame of the moving stationary solutions $\xi=z$, $\tau=t-z/v$, and the abbreviations

$$\hat{L}_{0f}=\hat{L}_0+h,\quad \hat{L}_{1f}=\hat{L}_1+h,\quad h=4f\cos q\sin^2\frac{Q}{2},$$

where $\hat{L}_0=\lambda^2/2-\frac{1}{2}\partial_{\tau\tau}-g^2$, $\hat{L}_1=\lambda^2/2-\frac{1}{2}\partial_{\tau\tau}-3g^2$ are the well-known Schrödinger type self-conjugated operators. It follows from Eq. (11) that the stability of the solution (9) can be inferred from the eigenvalue problem

$$\hat{L}_{0f}\hat{L}_{1f}a=p^2a\quad \text{or}\quad \hat{L}_{1f}\hat{L}_{0f}b=p^2b, \tag{12}$$

where $p^2=(K+2f\sin q\sin Q)^2$. As for $q=0$ [22] the eigenvalues can be found by solving the minimization problem

$$p^2=\min\left\{\frac{\langle\Psi|\hat{L}_{1f}|\Psi\rangle}{\langle\Psi|\hat{L}_{0f}^{-1}|\Psi\rangle}\right\} \tag{13}$$

and the solution (9) turns out to be likewise modulationally unstable for

$$\frac{8}{3}f\cos q\sin^2\frac{Q}{2}<\lambda^2 \tag{14}$$

provided that $\cos q>0$. However, this variational approach does not provide information about the MI gain and fails completely for $\cos q<0$.

To overcome these difficulties we use the perturbation theory near neutrally stable modes. This approach was successfully applied in continuous problems, viz., in the stability analysis of combustion waves [25], the oscillation spectrum of vortex filaments in liquid helium [26], solitons in media with weak dispersion [27], and solitons in plasma physics [4]. Here this approach can be used provided that $h\ll\lambda^2$. This constraint can be met for two situations, namely, (i) weak linear coupling between the guides in the array ($f\ll\lambda^2$) and arbitrary $q$ and $Q$ or (ii) strong coupling ($f\approx\lambda^2$), but modulation with a small spatial frequency $Q$ or/and an almost vanishing ''diffraction'' ($\delta q=|q-\pi/2|<<1$).

The idea of this approach was put forward in [25] and consists in looking for particular modes in the spectrum provided by Eq. (12), viz., those with the eigenvalue $p=0$ for a perturbation characterized by $h=0$. These perturbations correspond to neutrally stable modes which describe infinitesimal variations of the parameters of the stationary solution. Now, if $h$ is small the eigenfunctions and eigenvalues slightly differ from those of the neutrally stable modes. In our scenario the unperturbed solutions define an array of noninteracting identical Schrödinger solitons the phase of which rotates where the period is given by $2\pi/q$. The unperturbed problem (12) ($h=0$) yields the neutrally stable modes ($p=0$) [4]:

$$a_0^+=-2\frac{\partial g}{\partial\lambda^2},\quad a_0^-=\frac{\partial g}{\partial t},\quad b_0^+=g,\quad b_0^-=-tg, \tag{15}$$

where the $\pm$ signs correspond to even and odd eigenfunctions, respectively. Now making use of Eq. (15) as a zero approximation the eigenfunctions $a^\pm$ and $b^\pm$ as well as the corresponding eigenvalues $p^\pm$ can be expanded in terms of the small parameter $h$ as

$$a^\pm=\sum_{i=0}a_i^\pm,\quad (p^\pm)^2=\sum_{i=1}(p_i^\pm)^2. \tag{16}$$

Substituting Eq. (16) into Eq. (12) and taking into account terms up to the second order in $h$ we get for the eigenvalues

$$(p^+)^2=-2h\lambda^2+\frac{4}{3}\left(\frac{\pi^2}{3}+1\right)h^2, \tag{17}$$

$$(p^-)^2=\frac{2}{3}h\lambda^2+\frac{4}{9}\left(\frac{\pi^2}{3}-1\right)h^2. \tag{18}$$

As follows from Eqs. (17) and (18), either $(p^+)^2$ or $(p^-)^2$ is less than zero and the respective quantity $P^\pm=-ip^\pm$ represents the MI gain. For $0\leqslant q<\pi/2$ MI shows up for an even perturbation whereas for $\pi/2<q\leqslant\pi$ an odd perturbation leads to instability. These two types of MI may have different physical consequences, as we are going to show later.

Provided that the coupling is weak the MI gain in the discrete system can be easily calculated for any wave vector $Q$ of the perturbation. As can be seen from Eqs. (17) and (18), the maximum gain is reached near the edge of the Brillouin zone. If we omit second order terms in Eqs. (17) and (18) we find that $P^\pm=P_m^\pm|\sin(Q/2)|$ with

$$P_m^+=2\lambda\sqrt{2f\cos q} \tag{19}$$

and

$$P_m^-=2\lambda\sqrt{\frac{2}{3}f|\cos q|} \tag{20}$$

as the maximum values at $Q_m = \pm\pi$. If one takes into account second order terms in Eqs. (17) and (18) $|Q_m|$ decreases.

Finally, a remark is in order. Namely, in the continuous medium soliton stability with respect to transverse perturbations can be investigated only within the long-wavelength limit. In this case the MI gain grows with $Q$ and reaches its maximum for wave vectors $Q$ where the perturbation theory must not be applied. Thus it is impossible to identify the boundaries of the instability region as well as the maximum MI gain by using the perturbation theory [4].

Having identified the parameter space where MI exists we are now going to study the behavior of the unstable soliton array (9) beyond the initial stage of exponential growth by numerically solving the system (1). For the numerical calculations the split-step method using the fast-Fourier-transform algorithm (see e.g., [7], and references therein) with up to 128 temporal grid points was applied. An array of $N=16$ channels with periodical boundary conditions was considered. The perturbation applied contains even and odd temporal components, viz., $a=0.01\cos(Qn)[\gamma_1\cos\lambda t+\gamma_2\sin\lambda t]$ where $\gamma_{1,2}=0$ or 1. It turned out that the results practically did not change if the perturbation was localized at the solitons or not. As mentioned above, there are two different cases of MI which appear for $\cos q<0$ and $\cos q>0$. The former instability provokes a bending of the initially homogeneous soliton array, i.e., the soliton velocities are modulated across the waveguide array. This is displayed in Figs. 5(a)–5(c) for a transverse wave vector $q=\pi$, $\gamma_1=\gamma_2=1$, and for different wave vectors $Q$ of the perturbation for moderate propagation distances. The changes in the velocity are approximately proportional to $|\sin Q/2|\cos Qn$, which is in agreement with Eqs. (17) and (19). The omission of the even part of the perturbation ($\gamma_1=0$) does not change the results.

A different kind of evolution can be observed for $\cos q>0$ where the case $q=0$ is shown in Fig. 6. The even part of the perturbation now causes an energy redistribution between the waveguides as shown in Fig. 6(a). The initially homogeneous soliton array is modulated with the period $2\pi/Q$ as could be anticipated. This effect is known from plasma physics and is called there soliton bunching [4]. Eventually it may lead to the formation of compressed pulses localized in a few waveguides [20–22]. But for moderate distances and weak coupling ($f=0.1$) the system behaves almost periodically, i.e., we observed some kind of recurrence phenomenon between two spatial energy distributions shown in Figs. 6(a) and 6(b) [where Fig. 6(b) displays the most delocalized distribution]. In Figs. 7(a) and 7(b) the same patterns are shown for the case of $q=\pi/4$. We may again identify a considerable energy localization in a few channels [Fig. 7(a)] but with regard to the subsequent evolution an important difference to the previous case shows up. After having attained a weakly localized state [Fig. 7(b)] the system exhibits a recurrence to the energy distribution similar to that shown in Fig. 7(a), but the whole pattern slightly moves across the NOWA. For instance, the succeeding highly localized state appears for $z=13.5$ but shifted by $n=2$. Thus we can conclude that a nonvanishing transverse wave vector $q\neq 0$ (with $\cos q>0$) provokes a motion of the pulses across the array. In conjunction with ''bunching'' it evokes an energy switching between different channels.

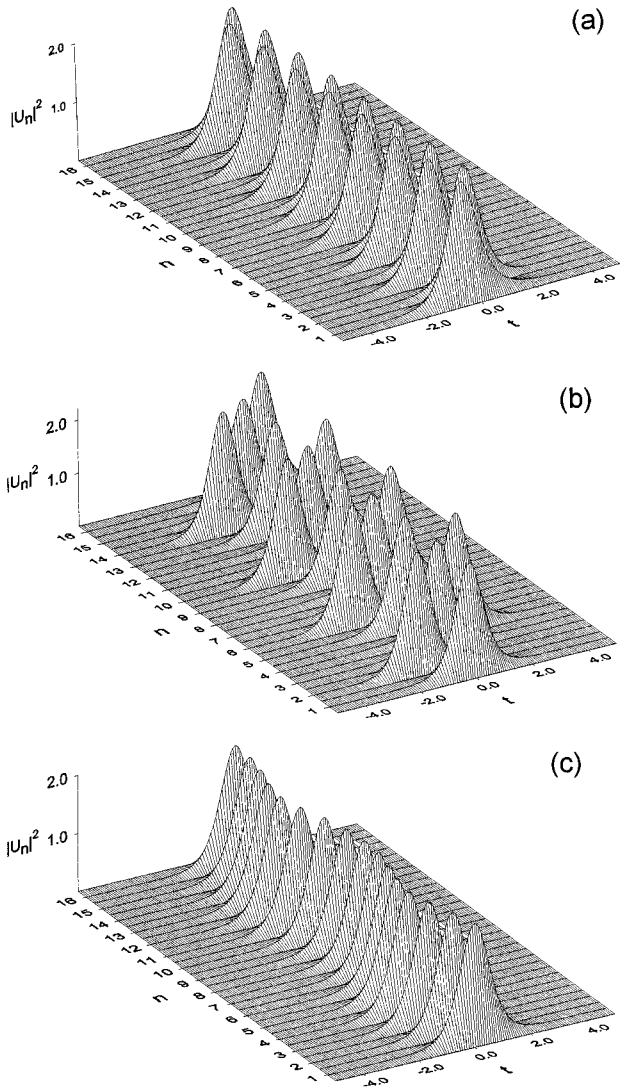


FIG. 5. Temporal field shape in the waveguide array after propagation distance $z$ (soliton bending). Parameters: $q=\pi$, $\lambda^2=2$, $f=0.1$, and (a) $Q=\pi$, $z=7$; (b) $Q=\pi/2$, $z=12$; (c) $Q=\pi/4$, $z=16$. $n$ labels the waveguide number.

For the particular situation $q=\pi/2$ (''diffractionless'' case) the solitons propagated like almost noninteracting, fairly stable entities.

This critical dependence of the evolution of unstable solutions on the transverse wave vector $q$ was previously identified for two- and three-core arrays by using a soliton perturbation theory [28,29]. In particular, for $q=0$ solitons attract each other and form a bound state whereas for $\cos q<0$ they repel. Moreover, for a three-core array and $q=0$ there is an energy flow from the outermost fibers to the central one. This flow is proportional to $(fz)^2$ in the initial stage of evolution and resembles the bunching effect [29].

## IV. CONCLUSIONS

In conclusion, we have studied the stability of moving continuous waves and rotating solitons in a nonlinear waveguide array against small modulations. For the cw case the domain as well as the gain of MI are analytically obtained. It

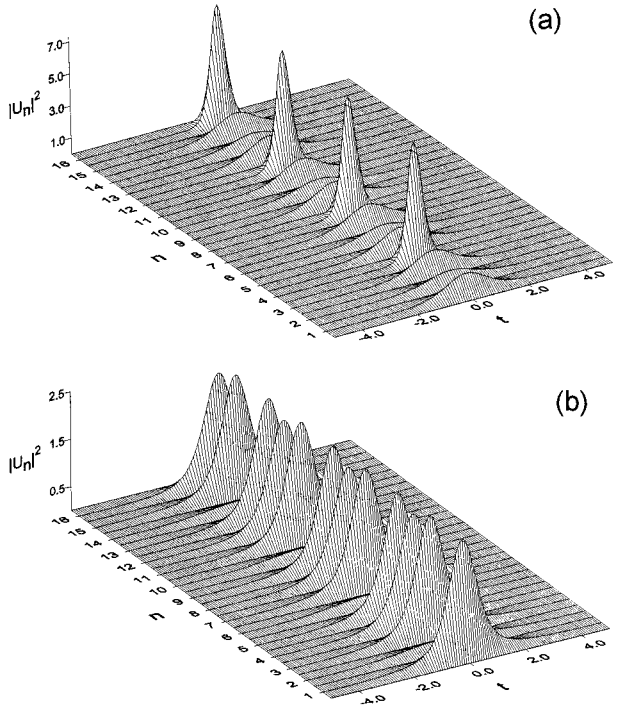


FIG. 6. Temporal field shape in the waveguide array after propagation distance $z$ (soliton bunching). Parameters: $q=0$, $Q=\pi/2$, $\lambda^2=2$, $f=0.1$, (a) $z=6.4$, (b) $z=8.3$.

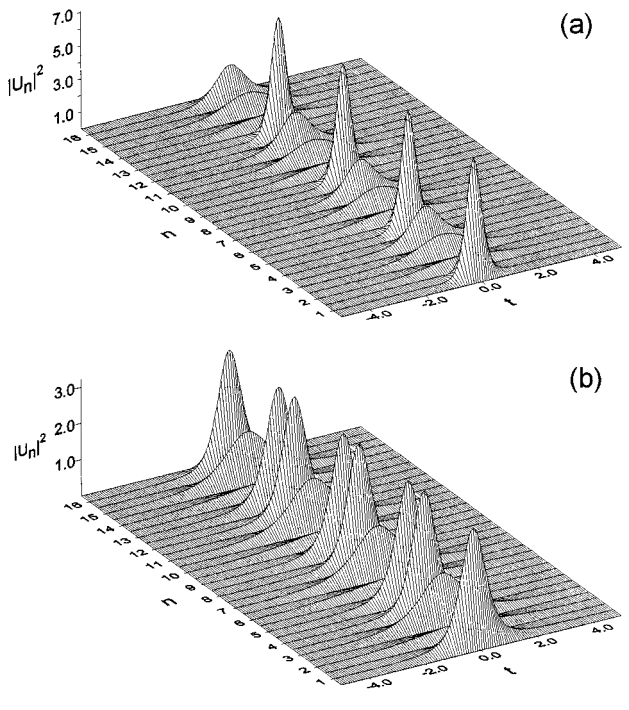


FIG. 7. Temporal field shape in the waveguide array after propagation distance $z$ (soliton bunching and shift, see text). Parameters: $q=\pi/4$, $Q=\pi/2$, $\lambda^2=2$, $f=0.1$, (a) $z=7.8$, (b) $z=9.5$.

turned out that both quantities exhibit a strong dependence on the transverse wave vector of the stationary solution. This dependence is not surprising because the transverse wave vector determines physically the kind of ''diffraction'' taking place in the array. The diffraction can attain either sign and can even be zero, which clearly underlines the peculiarities of these discrete systems with regard to continuous ones. The introduction of a nonzero transverse wave vector for an array of solitons corresponds to a rotation of the phase. By means of a perturbation theory near neutrally stable modes the MI gain is calculated. Again there were different solutions depending on the nature of diffraction. For the conventional, positive diffraction we obtained a soliton bunching where the amplitude modulation in the NOWA is determined by the wave vector of the perturbation. This scenario can eventually lead to a strong compression and localization. This corresponds to the collapse in the continuous model [21,22]. For negative diffraction the solitons in the array get a velocity rather than an amplitude modulation (soliton bending). Again the modulation period depends on the wave vector of the perturbation. The approach used here can be applied to modified versions of the discrete NLSE, e.g., to the case of an arbitrary nonlinearity $F(|U_n|^2)$ or linearly inhomogeneous arrays.

## ACKNOWLEDGMENTS

S.D. and F.L. gratefully acknowledge a grant from ''Deutche Forschungsgemeinschaft'' in the framework of the initiative ''Optical signal processing.'' I.R. gratefully acknowledges financial support from the ''Otto-Benecke Stiftung.''

[1] T. B. Benjamin and J. F. Feir, J. Fluid Mech. **27**, 417 (1967).
[2] V. I. Bespalov and V. I. Talanov, Pis'ma Zh. Éksp. Teor. Fiz. **3**, 471 (1966) [JETP Lett. **3**, 307 (1966)].
[3] H. C. Yuen and B. M. Lake, in *Soliton in Action*, edited by K. Lonngren and A. Scott (Academic Press, New York, 1978).
[4] E. A. Kuznetsov, V. E. Zacharov, and A. M. Rubenchik, Phys. Rep. **142**, 103 (1986).
[5] C. Montes, O. Legrand, A. M. Rubenchik, and I. V. Relke, in *Nonlinear World* (World Scientific, Singapore, 1990), p. 1250.
[6] F. Abdullaev, S. Darmanyan, and P. Khabibullaev, *Optical Solitons* (Springer-Verlag, Heidelberg, 1993).
[7] G. P. Agrawal, *Nonlinear Fiber Optics* (Academic Press, San Diego, 1995).
[8] A. Hasegawa, Opt. Lett. **9**, 288 (1984).
[9] K. Tai, A. Hasegawa, and A. Tomita, Phys. Rev. Lett. **11**, 171 (1986); Phys. Rev. A **46**, 3198 (1992).
[10] Yu. S. Kivshar and M. Peyrard, Phys. Rev. A **46**, 3198 (1992).
[11] V. M. Burlakov, S. A. Darmanyan, and V. N. Pyrkov, Phys. Rev. B **54**, 3257 (1996).
[12] D. N. Christodoulides and R. I. Joseph, Opt. Lett. **13**, 794 (1988).
[13] Yu. Kivshar, Opt. Lett. **18**, 1147 (1993).
[14] A. Aceves, C. De Angelis, T. Peschel, R. Muschall, F. Lederer, S. Trillo, and S. Wabnitz, Phys. Rev. E **53**, 1172 (1996).
[15] C. Schmidt-Hattenberger, U. Trutschel, and F. Lederer, Opt. Lett. **16**, 294 (1991).

[16] C. Schmidt-Hattenberger, R. Muschall, F. Lederer, and U. Trutschel, J. Opt. Soc. Am. B **10**, 1592 (1993).
[17] W. Krolikowski, U. Trutschel, M. Cronin-Golomb, and C. Schmidt-Hattenberger, Opt. Lett. **19**, 320 (1994).
[18] R. Muschall, C. Schmidt-Hattenberger, and F. Lederer, Opt. Lett. **19**, 323 (1994).
[19] W. Krolikowski and Yu. Kivshar, J. Opt. Soc. Am. B **13**, 876 (1996).
[20] A. V. Aceves, C. De Angelis, A. M. Rubenchik, and S. K. Turitsyn, Opt. Lett. **19**, 329 (1994).
[21] A. V. Aceves, G. G. Luther, C. De Angelis, A. M. Rubenchik, and S. K. Turitsyn, Phys. Rev. Lett. **75**, 73 (1995).
[22] A. V. Aceves, C. De Angelis, G. G. Luther, and A. M. Rubenchik, Opt. Lett. **19**, 1186 (1994).
[23] E. W. Laedke, K. H. Spatschek, S. K. Turitsyn, and V. K. Mezentsev, Phys. Rev. E **52**, 5549 (1996).
[24] A. Buryak and N. Akhmediev, IEEE J. Quantum Electron. **31**, 682 (1995).
[25] G. I. Barenblatt and Ya. B. Zel'dovich, Prikl. Mat. Mekh. **21**, 856 (1958).
[26] L. P. Pitaevski, Zh. Eksp. Teor. Fiz. **40**, 646 (1960) [Sov. Phys. JETP **13**, 451 (1961)].
[27] B. B. Kadomtsev and V. I. Petviashvili, Dokl. Akad. Nauk SSSR **192**, 753 (1970) [Sov. Phys. Dokl. **15**, 539 (1970)].
[28] F. Abdullaev, R. Abrarov, and S. Darmanyan, Opt. Lett. **14**, 131 (1989).
[29] R. Abrarov, P. Christiansen, S. Darmanyan, A. Scott, and M. Soerensen, Phys. Lett. A **171**, 298 (1992).